An Ytterbium doped monomode fiber laser: amplified spontaneous emission, modelisation of the gain and tunable operation

Sylvain Magne, Michel Druetta, Jean-Pierre Goure, Jean Claude Thevenin, Pierre Ferdinand, Gérard Monnom

An ytterbium-doped monomode fiber laser: amplified spontaneous emission, modeling of the gain and tunability in an external cavity

S. Magne[a,b]*, M. Druetta[a], J.P. Goure[a], J.C. Thevenin[b], P. Ferdinand[b], G. Monnomc

[a] Laboratoire Traitement du Signal et Instrumentation, URA CNRS 842, 23, rue du Dr Paul Michelon, F42023 St. Etienne, France

[b] Laboratoire de Mesures Optiques, LETI-DEIN, Bâtiment 94, CEA CEN Saclay, F 91191 Gif sur Yvette, France

[c] Laboratoire de Physique de la Matière Condensée, URA CNRS 190. Parc Valrose, F 06108 Nice, France

Abstract

The spectral behavior of the amplified spontaneous emission of an ytterbium-doped monomode fiber is described and the site-selective excitation tunability is explained. Then, the fiber gain is modeled, taking into account the fiber length and the pumping wavelength to optimize a three-level scheme room-temperature laser operation at 976 nm.

1. Introduction

In this paper, we describe the spectral behavior of the amplified spontaneous emission (ASE) in an ytterbium-doped fiber. We transpose the ASE line-narrowing model of Casperson and Yariv in order to check its validity for doped fibers. The expressions of fiber gain and the optimal length are recalled. Then, we show that there is a compromise between achieving a high population inversion and a low pumping power and that there is consequently an optimal pumping wavelength. Conversely, the pumping wavelength can be chosen in order to adjust the fluorescence spectrum, disregarding pumping efficiency considerations. The site-selective excitation (yielding a very broad tunability) has never been explained before and is explained by considering a fluorescence line narrowing (FLN) symbolic energy level diagram. Finally, tunable three-level laser action is demonstrated, taking into account all these considerations.

2. Theory

The fluorescence spectrum corresponds to different homogeneous contributions weighted by the Boltzmann distribution and inhomogeneously broadened due to site to site variation of the electric ligand field. At room temperature, only two of the four Stark levels of $^2F_{7/2}$ are resolved in fluorescence (Fig. 1).

Below saturation of the laser transition, the amplified spontaneous emission line narrowing is described by the relation [1]

$$\frac{\Delta\nu}{\Delta\nu_{inh}} = \frac{1}{\sqrt{g_0}} \qquad (1)$$

where $\Delta\nu_{inh}$ is the inhomogeneous linewidth measured from the absorption spectrum,

$\Delta\lambda_{inh} = c\frac{\Delta\nu_{inh}}{\nu^2} = 10$ nm. $\Delta\nu$ is the ASE-narrowed linewidth and g_0 is the unsaturated gain of the fiber laser (integrated along its length *L)* at the center of the gain profile $g(\lambda)$. This gain can be derived from the following formula [2]:

$$g(\lambda) \approx -\alpha_a(\lambda)\,\eta_s\,L + \left(1 + \frac{\sigma_e(\lambda)}{\sigma_a(\lambda)}\right)\frac{\sigma_a(\lambda)}{\sigma_p}\,\frac{F}{\eta_p}\,\frac{P_{abs}}{P_{sat}}\,\xi \qquad (2)$$

where η_s, η_p and F are guiding parameters of the fiber, $\sigma_a(\lambda)$, $\sigma_e(\lambda)$ and $\sigma_p(\lambda)$ are the interaction cross-sections of absorption [$^2F_{7/2} \rightarrow {}^2F_{5/2}(1)$], emission [$^2F_{5/2}(1) \rightarrow {}^2F_{7/2}$], and pump

[$^2F_{7/2}$ (1) $\rightarrow$ $^2F_{5/2}$ (2),(3)], respectively, α_a is the absorption coefficient of the laser transition and P_{abs} is the absorbed pump power (measured by the cut-back method). P_{sat} is the pump saturation power, defined as $P_{sat} = I_{sat}\,\pi\,W_p^2$, where I_{sat} is the pump saturation intensity at frequency ν_p, $I_{sat} = h\,\nu_p\,\sigma_p\tau$, and W_p is the pump mode waist. $\sigma_p(\lambda)$ ranges from 840 nm to around 940 nm. ξ is very close to unity for the ytterbium-doped fiber laser [2].

The peak stimulated emission cross-section was estimated using the modified Fuchtbauer Ladenburg equation and yielded 1.8×10^{20} cm^2 at 976 nm.

An optimized laser action requires choosing the pumping wavelength and the fiber length, key parameters in fiber laser behavior.

2.1 Fiber length optimization

The laser transition operating in a three-level laser scheme suffers reabsorption losses from the ground state, while the laser transition operating in a four-level laser scheme presents a smaller reabsorption loss provided that only 4% of the total population is in the Stark level (2) of $^2F_{7/2}$ (at room temperature). Therefore, the gain of the three-level scheme laser reaches a maximum at an optimal length, and the threshold of the fiber laser reaches a minimum at this same length. The fiber laser operates better in a "three-level" scheme for interaction lengths shorter than the optimal length and in a "four-level" scheme otherwise. In this latter scheme, the gain spectrum shifts towards longer wavelengths as the length increases beyond the optimal length owing the reabsorption from the ground state manifold.

The pump power decreases as the pump beam propagates along the fiber so that the local gain (in dB) decreases until finally reaching a null value at the optimal length defined by [2, 3]

$$P_p\left(L_{opt}\right) = \frac{\sigma_a(\lambda)}{\sigma_e(\lambda)}\,\frac{\eta_s}{F}\,P_{sat} \qquad (3)$$

where $P_p\left(L_{opt}\right)$ is the residual pump power at the optimal length. This optimal length can be determined by solving numerically (fourth-order Runge Kutta method) the equation of the pump mode evolution [2, 3], using a Gaussian approximation for the fundamental guided mode,

$$\frac{\mathrm{d}P_p(z)}{\mathrm{d}z} = \alpha_p\,P_{sat}\,\ln\left(\frac{1+[P_p(z)/P_{sat}](1-\eta_p)}{1+P_p(z)/P_{sat}}\right) \qquad (4)$$

These two simple formulae are valid since the pump transition is mainly homogeneously broadened, with a pumping yield close to unity. Though site-selective excitation is clearly seen, this is indeed the case, because the homogeneous linewidth far exceeds its inhomogeneous counterpart at room temperature (pump levels correspond to the upper Stark levels which are characterized by a high non-radiative rate within the upper level manifold

2.2 Pump wavelength optimization

The pumping wavelength can be chosen either to maximize the efficiency of the fiber laser or to adjust the fluorescence spectrum (Fig. 1) (disregarding pumping efficiency considerations). As the excitation wavelength is detuned from the absorption peak, the required pump power increases as P_{sat} increases. Furthermore, the maximum population inversion is set by the stimulated emission occurring on the pump transition $^2F_{7/2}$ (1) $\leftrightarrow$ $^2F_{5/2}$ (3), when pump photons induce as many transitions upwards (absorption) as downwards (stimulated emission). In thermal equilibrium, each Stark level of the upper-level manifold is filled according to Boltzmann statistics, so that, the higher the pump Stark level, the lower its thermal population and the higher its pumping yield. This latter condition counterbalances the need to excite the

top of the absorption band. Consequently, the pumping band is detuned from the absorption peak towards lower wavelengths [where Eqs. (2), (3) and (4) are satisfied].

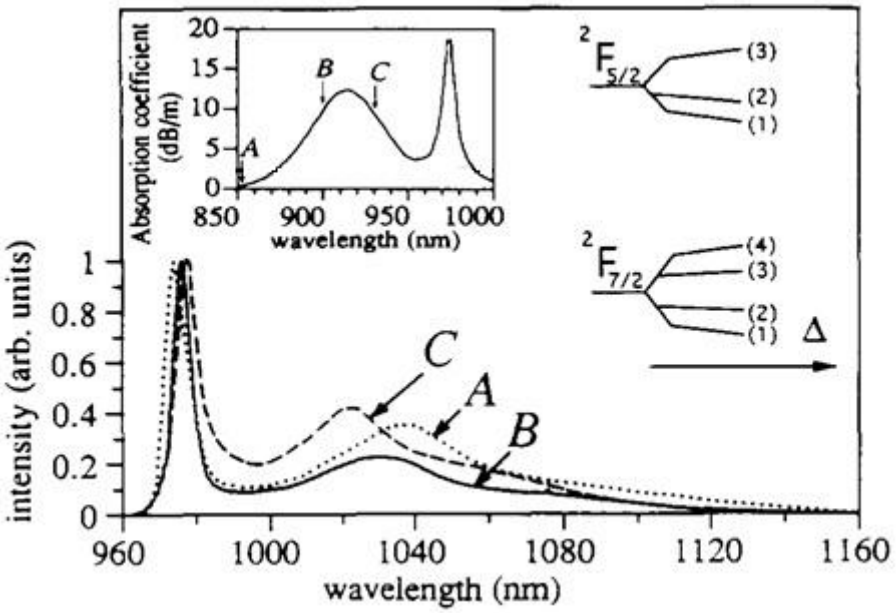

Fig. 1. Site-selective room-temperature fluorescence spectra (normalized to unity) of the monomode Yb^{3+} -doped fiber for several excitation wavelengths The fiber length is very short (3 cm) to prevent amplified spontaneous emission line narrowing. Inset shows the room temperature fiber absorption spectrum and the energy level fluorescence line narrowing symbolic diagram relative to the site distribution Δ. The fluorescence spectra are labeled according to their excitations located on the absorption spectrum.

3. Experiment

The silica fiber was fabricated with GeO_2-P_2O_5-SiO_2 core host glass by the Modified Chemical Vapor Deposition (MCVD) technique [3]. The laser doping with Yb_2O_3 was made by the solution doping method. The $^2F_{5/2}$ excited-state lifetime (Fig. 1) was determined by the fluorescence decay curves measurement and is 0.97 ms. The laser dopant concentration was determined by Neutron Activation Analysis (NAA) to be 85 ppm molar ± $5Yb_2O_3$ [3].

3.1 Amplified spontaneous emission behavior

A beveled facet at the output end of the fiber suppresses back reflections and prevents lasing. As the laser transition is very inhomogeneously broadened, the ASE spectra reveal reabsorptions that vary among different sites (Fig. 2). As the pumping and ASE power grow, the ASE spectrum shifts towards longer wavelengths and its width decreases to 2.5 nm.

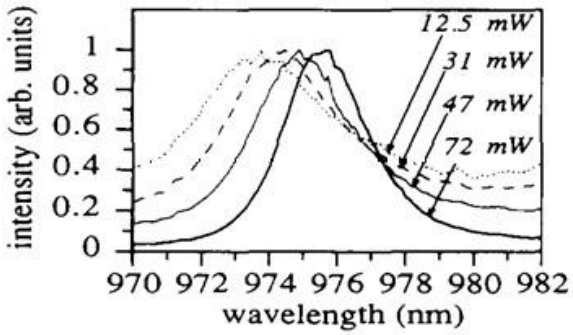

Fig. 2. Amplified spontaneous emission spectra at 976 nm (excitation at 900 nm) for several absorbed pump powers (the fiber is l.7 m long).

The ASE power remains below the laser saturation power (estimated to be around 700 µW) so that we cannot saturate the laser transition, even at high pumping powers (100 mW injected), in this single-pass configuration. In complete contrast to the ASE power behavior, the saturation is easily reached in broadband laser action with bare fiber output ends (4% reflection), with about 50% laser efficiency. In contrast to the ASE line narrowing (below saturation), we observe a rebroadening laser spectrum beyond saturation, as predicted [1].

The comparison between the experimental and calculated line narrowing is shown in Table 1. Some discrepancies remain, which can be attributed to the longitudinal evolution of the local gain, ground state reabsorptions and saturation of the gain by the four-level scheme amplified spontaneous emission. This latter explanation can account for the larger discrepancies observed for higher lengths.

Fiber legth 1.2 m		Fiber length 1.7 m	
experiment	calculation	experiment	calculation
3.7	3.9	4.1	6.5
3.3	3.4	3.6	2.6
2.9	2.5	3.3	2
2.7	2.4	2.9	1.6

Table 1. Comparison between experimental and calculated ASE linewidths at 976 nm

3.2. Tunability in an external cavity

As the pumping wavelength decreases, the sites corresponding to upper Stark level energies are predominantly excited and the thin fluorescence peak shifts towards smaller wavelengths from 978 nm to 974 nm while the broad peak shifts towards higher wavelengths from 1020 to 1040 nm (Fig. 1). The symbolic energy level diagram explains the site-selective excitation tunability well. Pump ground state absorption occurs between energy levels $^2F_{7/2}$ (1) and $^2F_{5/2}$ (3), followed by a non-radiative relaxation to the lower level (1) of $^2F_{5/2}$ and the fluorescence is thus observed in a non-resonant way [4].

When the excitation wavelength is around 850 nm (see arrow A in Fig. 1). the sites corresponding to the right part of the diagram are predominantly excited (the interaction with the homogeneous profile of the other sites is less efficient). The fluorescence of the $^2F_{5/2}$ (1)→ $^2F_{7/2}$ (1) transition (three-level laser scheme) is then shifted to higher energies (i.e. lower wavelengths) whereas the fluorescence of the transitions $^2F_{5/2}$ (1)→ $^2F_{7/2}$ (4), (3), (2) (four-level laser scheme) is then shifted to lower energies (i.e. higher wavelengths). The opposite behavior is observed as the excitation wavelength increases, because the energy shift between $^2F_{5/2}$ (1) and $^2F_{7/2}$ (4), (3), (2) increases whereas the energy shift between $^2F_{5/2}$ (1) and $^2F_{7/2}$ (1) decreases (arrow C in Fig. 1).

When conveniently pumped, the ytterbium-doped fiber laser can therefore provide a much larger tunability than its bulk crystalline counterparts, as previously described [5], at the expense of a lower extraction efficiency compensated for by the optical confinement.

A defined optimal length of 1.2 m of fiber (of 4 µm core diameter) was pumped (using an argon ion pumped titanium sapphire laser) at an optimal excitation wavelength of 900 nm, yielding both a high population inversion and a minimum pumping power. The cavity includes a dichroic mirror and an achromatic objective. A diffraction grating (2000 lines/mm).

at “Littrow configuration” and in grazing incidence, provided a very strong selective feedback, and a tunability of 3 nm was achieved around 976 nm, with 0.2 nm linewidth and a slope efficiency of 10%.

The slope efficiency decreases as the laser linewidth decreases on account of the large inhomogeneous broadening. Injection losses and the grating diffraction efficiency also considerably limit the lasing performance of the fiber laser.

4. Conclusions

Simple amplified spontaneous emission studies reveal the amplification behavior of the fiber laser and the main parameters of the fiber laser (pumping wavelength and fiber length) are detailed and optimized to achieve a continuous-wave tunable three-level laser operation.

The spectral evolution of the ASE three-level transition line narrowing is described by the model of Casperson and Yariv. Some discrepancies remain, which are attributed mainly to saturation by transitions corresponding to a four-level scheme. A useful pumping band extending from 840 to around 915 nm provides a site-selective excitation tunability, well explained by the fluorescence line narrowing symbolic energy level diagram.

References

[1] L.W. Casperson and A. Yariv, IEEE J. Quantum Electron. 8 (1972) 80.

[2] M.J.F. Digonnet, IEEE L. Quantum Electron. 26 (1990) 1788.

[3] S. Magne, PhD thesis, Université de Saint-Etienne (1993).

[4] M.J. Weber, in: Laser Spectroscopy of Solids, eds. W.M. Yen and P.M. Selzer (Springer, New York, 1981) p. 189.

[5] D.C. Hanna, R.M. Percival, I.R. Perry, R.G. Smart, P.J. Suni and A.C. Tropper, J. Mod. Optics 37 (1990) 517.